Enhanced climate change response of wintertime North Atlantic circulation, cyclonic activity and precipitation in a 25 km-resolution global atmospheric model

Enhanced climate change response of wintertime North Atlantic circulation, cyclonic activity and precipitation in a 25 km-resolution global atmospheric model

Alexander J. Baker[1,*], Reinhard Schiemann[1], Kevin I. Hodges[1], Marie-Estelle Demory[1], Matthew S. Mizielinski[2], Malcolm J. Roberts[2], Len C. Shaffrey[1], Jane Strachan[2], and Pier Luigi Vidale[1]

[1] National Centre for Atmospheric Science and Department of Meteorology, University of Reading, Reading, Berkshire, UK

[2] Met Office Hadley Centre, Exeter, Devon, UK

* alexander.baker@reading.ac.uk

Journal of Climate **– revised submission (JCLI-D-19-0054)**

Early Online Release: This preliminary version has been accepted for publication in *Journal of Climate*, may be fully cited, and has been assigned DOI 10.1175/JCLI-D-19-0054.1. The final typeset copyedited article will replace the EOR at the above DOI when it is published.

Abstract

Wintertime mid-latitude cyclone activity and precipitation are projected to increase across northern Europe and decrease over southern Europe, particularly over the western Mediterranean. Greater confidence in these regional projections may be established by their replication in state-of-the-art, high-resolution global climate models that resolve synoptic-scale dynamics. We evaluated the representation of the wintertime eddy-driven and subtropical jet streams, extratropical cyclone activity and precipitation across the North Atlantic and Europe under historical (1985-2011) and RCP8.5 sea surface temperature forcing in an ensemble of atmosphere-only HadGEM3-GA3.0 simulations, where horizontal atmospheric resolution is increased from 135 to 25 km. Under RCP8.5, increased (decreased) frequency of northern (southern) eddy-driven jet occurrences and a basin-wide poleward shift in the upper-level westerly flow are simulated. Increasing atmospheric resolution significantly enhances these climate change responses. At 25 km resolution, these enhanced changes in large-scale circulation amplify increases (decreases) in extratropical cyclone track density and mean intensity across the northern (southern) Euro-Atlantic region under RCP8.5. These synoptic changes with resolution impact the overall climate change response of mean and heavy winter precipitation: wetter (drier) conditions in northern (southern) Europe are also amplified at 25 km resolution. For example, the reduction in heavy precipitation simulated over the Iberian Peninsula under RCP8.5 is ~15% at 135 km, but ~30% at 25 km resolution. Conversely, a shift to more frequent high ETC-associated precipitation rates is simulated over Scandinavia under RCP8.5, which is enhanced at 25 km. This study provides evidence that global atmospheric resolution may be a crucial consideration in European winter climate change projections.

Accepted for publication in *Journal of Climate*. DOI10.1175/JCLI-D-19-0054.1.

1. Introduction

Across the Euro-Atlantic region, hazardous weather – particularly heavy precipitation and wind extremes – is primarily related to extratropical storm occurrence (e.g., Huntingford et al. 2014), which is modulated by variability in the westerly flow over the North Atlantic basin. Model projections of the behaviour of such dynamical phenomena under climate change are uncertain, but greater confidence could be established by running global climate models at resolutions sufficient to resolve weather-scale processes, and thereby internally-driven climate variability (Roberts et al. 2018), increasing understanding of Europe's future exposure to climate risk.

Synoptic conditions over the North Atlantic are governed by two jet streams: the upper-tropospheric subtropical jet, which arises from angular momentum transport by the Hadley circulation (Schneider 2006), and the lower-tropospheric eddy-driven jet, induced by eddy momentum flux from baroclinic waves (Hoskins 1983). The wintertime eddy-driven jet exhibits an observed tri-modal regime behaviour that is most pronounced during winter: southern (~35-40 °N), central (~42-58 °N) and northern (~53-60 °N) positions are occupied preferentially because transient eddy forcing acts to maintain the eddy-driven jet at a given latitude, and variability in this forcing causes meridional jet shifts (Woollings et al. 2010). Variability in this large-scale, zonal-mean circulation modulates weather regime frequency (Madonna et al. 2017) and steers mid-latitude, extratropical cyclone (ETC) tracks (Bengtsson et al. 2006; Della-Marta and Pinto 2009; Masato et al. 2016; Pfahl et al. 2017; Pinto et al. 2009; Zappa and Shepherd 2017). ETCs are synoptic-scale, low-pressure systems whose cyclogenesis, propagation (generally poleward and eastward), decay and cyclolysis occur within the mid-latitude storm track regions. ETC cyclogenesis occurs frequently over North America, where a strong meridional temperature gradient and thus high baroclinicity exists at

Accepted for publication in *Journal of Climate*. DOI10.1175/JCLI-D-19-0054.1.

the interface of subtropical and polar air masses (polar front). Subsequently, these synoptic disturbances develop into mature ETCs over the North Atlantic basin (Pinto et al. 2009). ETCs are important for the poleward transport of heat, moisture and momentum in the atmospheric general circulation, reducing the equator-to-pole energy imbalance (Kaspi and Schneider 2013; Schneider 2006; Shaw et al. 2016), but are also responsible for a substantial component of variability in winter precipitation and wind conditions across mid- and mid-to-high-latitude regions (Pfahl and Wernli 2012). The climatological mean contribution of ETCs to European winter precipitation is ~70% (Hawcroft et al. 2012) and model simulations indicate increased ETC-associated precipitation by the end of the 21st century (Hawcroft et al. 2018). Storm track processes are therefore crucial for European hydroclimate and extreme event variability.

On seasonal to decadal timescales, the North Atlantic Oscillation (NAO), the leading mode of natural variability in large-scale atmospheric circulation, storminess and precipitation across the Euro-Atlantic region (Pinto et al. 2009; Wallace and Gutzler 1981; Zveryaev 2004, 2006), is dominated by positional variability of the North Atlantic jet and storm track (Woollings et al. 2018). Therefore, the ability of global climate models to capture variability in North Atlantic zonal-mean flow and ETC occurrence is critical for climate impact studies and projections at the regional scale. However, many CMIP5 models are unable to capture the tri-modality of the North Atlantic eddy-driven jet (Iqbal et al. 2018). This highlights the importance of resolution sufficiency and of performing climate simulations at a horizontal resolution sufficient to resolve weather systems and their feedback on large-scale circulation and variability.

Accepted for publication in *Journal of Climate*. DOI10.1175/JCLI-D-19-0054.1.

There is evidence from both global and regional modelling studies that global atmospheric model resolution is important for representing the North Atlantic storm track, cyclonic activity and precipitation, indicating that resolution is an important modelling consideration in the climate change projection of these phenomena. Multi-model climate change projections from the 5th phase of the Coupled Model Intercomparison Project (CMIP5) show a decline in winter cyclonic activity and precipitation over southern Europe, particularly the western Mediterranean, and an increase over north-western Europe (Zappa et al. 2013b). Shepherd (2014) highlighted the non-robustness of the winter circulation response to climate change over the North Atlantic in global CMIP5 models, hypothesising that differing atmospheric model resolution is an important factor. Zappa et al. (2013a) showed that CMIP5 models with the best representation of the North Atlantic storm track are those of highest resolution within the CMIP5 ensemble, indicating that high atmospheric resolution is necessary to accurately capture the position and tilt of the North Atlantic storm track, as well as variability in the downstream impacts of North Atlantic storminess. Global EC-Earth simulations performed at resolutions of ~112 and ~25 km revealed resolution sensitivity of European precipitation due to the resolution sensitivity of the simulated North Atlantic storm track, particularly its more realistic tilt (van Haren et al. 2015). Global historical and future climate ECHAM5 simulations at equivalent resolutions of ~60 and ~40 km show that the responses of ETC intensity and wind speed maxima to warming are partly dependent on model resolution and, for both climates, the impact of resolution exceeds the climate change response at either resolution (Champion et al. 2011). These studies provide evidence that increases in atmospheric resolution improve simulated storm track dynamics.

To improve mean and extreme climate predictions, a quantitative assessment of the ability of global climate models to simulate weather-scale processes is required, but such processes are

Accepted for publication in *Journal of Climate*. DOI10.1175/JCLI-D-19-0054.1.

99 driven by relatively uncertain circulation dynamics (Woollings 2010; Zappa and Shepherd
100 2017). High model resolution is particularly important for Europe, a populous region where
101 synoptic systems interact with complex coastlines, orography and the Mediterranean Sea.
102 Global and regional modelling studies simulating present-climate precipitation have
103 demonstrated the resolution sensitivity of mean and extreme European precipitation due to
104 orography (Delworth et al. 2012; Prein et al. 2016; Schiemann et al. 2018) and models'
105 representation of the North Atlantic storm track (van Haren et al. 2015). Clearly, high-fidelity
106 model representations of boundary conditions, large-scale atmospheric circulation, storm
107 track processes, and synoptic phenomena are all key to simulating climate change patterns
108 across the Euro-Atlantic region, highlighting the value of global models. Current high-
109 performance computing and data management facilities now allow multi-decadal simulations
110 at effective resolutions adequate to resolve synoptic phenomena (Mizielinski et al. 2014; van
111 Haren et al. 2015; Zhang et al. 2016).
112
113 Overall, global and regional modelling efforts highlight the need to quantify the impact of
114 atmospheric resolution on North Atlantic circulation and hydroclimate in isolation by the
115 analysis of global climate model experiments designed to quantify the impact of resolution.
116 In this study, we have quantified the impact of increasing global atmospheric model
117 resolution on the response of Euro-Atlantic circulation, storminess and precipitation to
118 climate change. We focus on boreal winter (December-February; DJF), when mid-latitude
119 storm tracks are most active and the majority of precipitation occurs over the mid-latitude
120 North Atlantic. The representation of wintertime dynamics in climate models is important for
121 their simulation of other canonical seasons. For example, models' ability to capture
122 extratropical winter precipitation impacts their ability to simulate spring and summer soil
123 moisture levels and, in turn, droughts and heatwaves, highlighting the importance of

Accepted for publication in *Journal of Climate*. DOI10.1175/JCLI-D-19-0054.1.

accurately reproducing climatological cold season precipitation, its variability, and the dynamical phenomena with which it is associated (Hawcroft et al. 2016; Vidale et al. 2007). The aims of this study are: (i) to compare large-scale circulation, ETC activity and precipitation over the Euro-Atlantic domain simulated at 135 km, a resolution typical of CMIP5 GCMs, with that simulated at 60 and 25 km resolution; (ii) to identify regions where resolution impacts both the historical mean state and climate change response; (iii) to consider the implications for climate change impact studies for this region ahead of the 6th phase of the Coupled Model Intercomparison Project (CMIP6), particularly HighResMIP (Haarsma et al. 2016). To make this contribution, we analyse an ensemble of global historical and future climate model simulations from a single model, where only horizontal atmospheric resolution is increased. This allows us to isolate the role of atmospheric resolution without needing to account for inter-model disparities in formulation, complexity, or tuning, all issues that hinder resolution sensitivity studies (Matsueda and Palmer 2011). This paper continues with a description of the model ensemble, North Atlantic jet analysis techniques, and ETC tracking and analysis in section 2. Sequentially, we examine the impact of increased atmospheric model resolution under historical and RCP8.5 forcings on the North Atlantic zonal-mean circulation (section 3), ETC activity (section 4) and precipitation (section 5). We discuss these results in section 6 and summarise our conclusions in section 7.

2. Data and methods

2.1 Model ensemble

We analysed an ensemble of global atmosphere-only simulations performed with Hadley Centre Global Environmental Model (version 3) Global Atmosphere 3.0 (hereafter HadGEM3-GA3.0; Walters et al. 2011). These simulations are part of the UPSCALE (UK on

Accepted for publication in *Journal of Climate*. DOI10.1175/JCLI-D-19-0054.1.

PRACE: weather-resolving Simulations for globAL Environmental risk) project (Mizielinski et al. 2014), which offers an opportunity to evaluate the sensitivity of aspects of global and regional climate and their physical drivers to horizontal atmospheric resolution. UPSCALE simulations were performed for the period 1985-2011 at N96, N216 and N512 resolutions, where 'Nx' denotes global latitude and longitude grid of 1.5x+1 and 2x cells, respectively. Corresponding nominal mid-latitude grid spacings (at 50° latitude) are 135, 60 and 25 km, respectively. All simulations have 85 vertical levels and are forced by daily Met Office Operational SST and Sea Ice Analysis (OSTIA) data (Donlon et al. 2012), which were regridded from their native resolution of 1/20º to the three atmospheric resolutions (Fig. S1), and time-varying forcings were defined following AMIP-II protocols (Mizielinski et al. 2014). The historical climate ensemble size for the N96, N216 and N512 resolutions is five, three and five members, respectively. Future (end of the 21st century) climate change simulations were configured using a time-slice methodology forced by the OSTIA historical SST field plus the SST change between the periods 1990-2010 and 2090-2110 simulated by the HadGEM2 Earth System under the IPCC Representative Concentration Pathway 8.5 (RCP8.5) scenario. For regions experiencing sea ice loss under RCP8.5 forcing, SST values were interpolated from HadGEM2. At each resolution, three future climate ensemble members were run. Beyond minor adjustments to ensure numerical stability at each resolution, which are given in Mizielinski et al. (2014), no model retuning was performed (Demory et al. 2014).

For high-resolution global models, there is necessarily a trade-off between resolution and ensemble size, constrained by computational expense. Nevertheless, the UPSCALE project's experimental design – the combination of model resolution range, simulation length, availability of multiple ensemble members for better event sampling, and the lack of model

Accepted for publication in *Journal of Climate*. DOI10.1175/JCLI-D-19-0054.1.

retuning – allowed us to isolate the role of atmospheric resolution in the simulated historical climate and under RCP8.5.

2.2 Eddy-driven jet variability analysis

The action of transient eddy forcing to accelerate westerly winds occurs throughout the depth of the troposphere, but is particularly strong at low levels (Hoskins et al. 1983). The regime behaviour of the North Atlantic eddy-driven jet is examined in HadGEM3-GA3.0 following the method of Woollings et al. (2010). Daily zonal wind data were averaged over the 925, 850 and 700 hPa levels, then averaged zonally over a North Atlantic longitudinal sector (15-75 °N, 0-60 °W). The use of three rather than four levels does not significantly affect our results (see Supplementary information, section S1). A low-pass Lanczos filter (Duchon 1979) was applied with a cut-off value of 10 days to remove wind features associated with synoptic systems. The latitudes at which maxima of the resulting zonal-mean westerly wind profiles occur are defined as jet latitudes. Grid cells where orography exceeds 750 m were masked to avoid the inclusion of spurious sub-surface winds (e.g., over southernmost Greenland) in this analysis, particularly at the lowest isobaric level of 925 hPa (see Supplementary information). We also examined the inverse relationship between jet latitude variance and jet speed. Following Woollings et al. (2018), we computed the standard deviation of jet latitude binned by jet speed. We computed jet speed as the square root of the sum of the squares of the zonal and meridional winds, which accounts for instances when the magnitude of jet speed is dominated by the meridional component (e.g., due to jet meandering). To maximise sampling in these analyses, the low-pass-filtered wind time series for all ensemble members were concatenated for each resolution, taking advantage of the UPSCALE ensemble size. We compared model results for both of these analyses with the ERA5, ERA-Interim (Dee et al. 2011) and NCEP-CFSR (Saha et al. 2010) reanalyses for the

Accepted for publication in *Journal of Climate*. DOI10.1175/JCLI-D-19-0054.1.

period 1979-2016. All data were regridded to the N96 grid to isolate resolution sensitivity from any improved sampling at higher resolution.

2.3 Extratropical cyclone tracking

To identify and track the evolution of ETCs in this study, we used the objective feature-tracking algorithm – *TRACK* – of Hodges (1995, 1999), previously applied to reanalyses (Dacre and Gray 2013; Hawcroft et al. 2012; e.g., Hoskins and Hodges 2002) and model simulations of both present (e.g., Catto et al. 2010; Hawcroft et al. 2016) and future climates (e.g., Zappa et al. 2015; Zappa et al. 2013a). The Lagrangian *TRACK* algorithm was applied to 6-hourly, spectrally-filtered vorticity maxima at the 850 hPa level. Wavenumbers 0-5 and >42 are filtered out (i.e., truncation to T42 resolution, retaining wavenumbers 6-42), which excludes large-scale planetary motion and small-scale noise, respectively. Final ETC tracks represent only those identified features that propagate at least 1000 km and whose vorticity maxima exceed 1.0×10^{-5} s^{-1} and lifetime exceeds 2 days. These post-processing criteria exclude spurious stationary features in the vorticity field. Statistical ETC track density and mean intensity (as measured by vorticity) metrics were computed according to Hoskins and Hodges (2002) and compared with ERA-Interim reanalysis data for the period 1979-2016 (Dee et al. 2011).

2.4. Quantification of cyclone-associated precipitation

To associate precipitation to tracked ETCs, a radial cap was defined around each ETC centre at each 6-hourly timestep and precipitation within this cap is defined as cyclone-associated. The sensitivity of this analysis to cap radius was investigated by Hawcroft et al. (2012), who established the need to define cap radius according to the season and ocean basin in question. Accordingly, following Hawcroft et al. (2012) and Zappa et al. (2015; 2013a), we employed

Accepted for publication in *Journal of Climate*. DOI10.1175/JCLI-D-19-0054.1.

a constant cap radius of 10° in our analysis of wintertime North Atlantic ETCs, which is close to that used by Hawcroft et al. (2012) and minimises overlap between caps at a given timestep.

2.5 Significance testing

The statistical significance (above the 95 % level) of model-observation or inter-resolution (i.e., high- minus low-resolution) differences was determined with respect to interannual variability by applying Welch's unequal variances *t*-test.

3. Resolution sensitivity of Euro-Atlantic zonal-mean circulation under historical climate and RCP8.5

In this section, we evaluate the mean state of the eddy-driven and subtropical components of North Atlantic westerly flow simulated by HadGEM3-GA3.0 under historical and RCP8.5 SST forcings, focussing on the impact of increased atmospheric resolution.

3.1 North Atlantic eddy-driven jet

We compare the representation of the tri-modal regime behaviour of the wintertime North Atlantic eddy-driven jet latitude across the historical climate simulations with the ERA5, ERA-Interim and NCEP-CFSR reanalyses (Fig. 1). Overall, the tri-modal behaviour of the eddy-driven jet is captured by the historical HadGEM3-GA3.0 simulations at each of the three resolutions considered here. However, increasing resolution from N96 to N512 decreases the southern jet regime frequency (matching all three reanalyses more closely), increases the central regime frequency (exceeding the reanalyses), and causes a double-peak in the northern regime frequency, which is not present in the lower-resolution reanalyses or

Accepted for publication in *Journal of Climate*. DOI10.1175/JCLI-D-19-0054.1.

N96 simulations (Fig. 1, upper panel). This double-peak is, however, present in the latest ERA5 reanalysis, whose resolution (30 km) is comparable to N512, and is likely related to a better representation of orographic boundary conditions (i.e., Greenland and Iceland orography), known to influence where peaks in the wintertime frequency of low-level westerly jet events occur over the North Atlantic (Woollings et al. 2010). Despite the presence of a central peak bias at N512, increased resolution improves the overall frequency distribution of eddy-driven jet latitude and refines our view of northern regime behaviour arising from interaction with orography. Moreover, the observed inverse relationship between jet latitude variance and jet speed is well-captured (compared with all three reanalyses) across each model resolution under historical SST forcing (Fig. 2).

The latitudinal response of the eddy-driven jet to RCP8.5 in HadGEM3-GA3.0 is a pronounced poleward shift, shown clearly by zonally-averaged jet latitude probability density (Fig. 1, middle panel). At N96, the tri-modal jet latitude distribution is significantly different from the historical simulations, with a smoothing-out of the southern regime, a decrease in the peak frequency of the central regime, which also exhibits a broader shape, and an increase in the frequency of the northern regime. The southern regime response is further reduced at N216 and N512 resolutions. The northern regime response is increased markedly at N512 and also exhibits a double peak. Moreover, the inverse relationship between jet latitude variance and jet speed changes under RCP8.5 (Fig. 2). Jet latitude variability is reduced across all jet speed percentiles, with the largest such change simulated at N512. Overall, the probability density function of eddy-driven jet latitude is redistributed poleward (Fig. 1) and is less variable (Fig. 2) under RCP8.5, both responses forced by increased SST, which dominates jet shift in the Northern Hemisphere (Grise and Polvani 2014). These results indicate that increasing atmospheric resolution amplifies these behaviours under climate

Accepted for publication in *Journal of Climate*. DOI10.1175/JCLI-D-19-0054.1.

change, further discussion and interpretation of which is presented in the subsequent sections. Additionally, our results are consistent with Matsueda and Palmer (2011), who used the JMA-GSM model to show that coarse resolution (180 km) may underestimate the magnitude of the climate change response of North Atlantic westerly flow at 850 hPa, which is increased significantly by increasing resolution to 20 km.

3.2 North Atlantic subtropical jet

Historical HadGEM3-GA3.0 simulations capture the wintertime climatological upper-tropospheric (250 hPa) zonal wind field over the North Atlantic basin. Biases of up to ~4 ms^{-1} (versus ERA-Interim) over this region are statistically insignificant with respect to interannual variability, and particularly low over the poleward flank of the subtropical jet (Fig. S2). Additionally, a localised positive bias east of the Mediterranean Sea at N96 is reduced in spatial extent at N512. At N512, North Atlantic zonal flow exhibits a southwest-northeast tilt compared with the more zonal orientation simulated at N96 (Fig 3), which is likely due to the improved representation of orographic boundary conditions at this resolution (Fig. S3) allowing more realistic simulation of westerly flow incident on the Rocky Mountains. Increasing resolution also enhances the zonal wind over northern Europe and reduces it over south-eastern Europe, resembling a positive winter NAO-like pattern (Fig. 3). Over the North Atlantic, dipolar patterns of opposite sign are seen in the N216-N96 and N512-N216 difference maps, but these differences are largely statistically insignificant at the 95 % level.

The RCP8.5 response of the upper-tropospheric zonal wind field over the North Atlantic simulated by HadGEM3-GA3.0 is a pronounced basin-wide poleward shift and eastward extension (Fig. 4). This response is enhanced when resolution is increased in HadGEM-

Accepted for publication in *Journal of Climate*. DOI10.1175/JCLI-D-19-0054.1.

GA3.0 from N96 to N512, particularly over the eastern North Atlantic and Mediterranean basin. This spatial pattern of resolution sensitivity for N512-N96 resembles that of the historical climate (Fig. 3), indicating that the resolution sensitivity of the mean state zonal flow may impact that of the climate change response. Vertical (latitude-height) sections of the zonal wind field, averaged over the eastern Atlantic (0-40 °W), show this northward shift is simulated throughout the troposphere (Fig. 5). Under RCP8.5, the region wherein zonal wind speed at 250 hPa exceeds 30 ms^{-1} extends further east over the north-eastern North Atlantic than under historical climate forcing. At N216 and N512, this north-eastward extension towards northern Europe is enhanced; that is to say, these high wind speeds are projected to occur further east over Europe at increased resolution (Fig. S4), indicating upper-level, subtropical jet extension as resolution is increased from N96 to N512.

We undertook a correlation analysis to establish whether changes in the wintertime tropical Atlantic Hadley circulation response to RCP8.5 with resolution could provide more insight into the resolution-dependence of the subtropical jet response under RCP8.5. Specifically, we correlated inter-seasonal variability in tropical Atlantic vertical velocity (i.e., Lagrangian tendency of atmospheric air pressure, ω, at 500 hPa) with zonal wind. However, this analysis (not shown) revealed no evidence for a tropical cause of the resolution-dependent behaviour of North Atlantic zonal flow seen in these HadGEM3-GA3.0 integrations. While this analysis alone does not rule out any influence of the tropics, we limit the scope of this study to an examination of the consequences of a resolution-dependent flow response to warming for storm track phenomena and precipitation, focussing on significant differences between N96 and N512 resolutions.

Accepted for publication in *Journal of Climate*. DOI10.1175/JCLI-D-19-0054.1.

4. Resolution sensitivity of extratropical cyclone activity under historical climate and RCP8.5

ETCs, steered by the atmospheric flow over the North Atlantic, are primarily responsible for high-impact weather – namely, strong wind and heavy precipitation events – downstream over Europe (Madonna et al. 2017). Strengthened upper-level winds over the North Atlantic may increase the meridional propagation of mid-latitude cyclonic systems (Tamarin-Brodsky and Kaspi 2017) and, given the results presented in section 3, we therefore expect ETC activity simulated by HadGEM3-GA3.0 to change with resolution. To quantify this, we evaluated Euro-Atlantic ETC activity simulated by HadGEM3-GA3.0 under historical and RCP8.5 SST forcings.

An ensemble-mean HadGEM3-GA3.0 bias in ETC track density (versus ERA-Interim data; Fig. S5) of ~15% at N96 resolution is statistically significant only in a confined region of the North and Norwegian Seas, and this bias is reduced to ~7% at N512. This improvement of simulated ETC activity with increased resolution highlights the necessity of resolving synoptic phenomena in studies of wintertime European hydroclimate. For the historical climate, HadGEM3-GA3.0 simulates higher ETC track density at N512 across the downstream region of the North Atlantic storm track, Scandinavia and the Iberian Peninsula than at N96 (Fig. 6). Climatologically, ~1 to ~3 additional cyclones per month per unit area (5^{o} radial cap) are simulated over these regions at N512 compared with N96. The increases with resolution over Iberia and northwest Africa, where absolute values at N96 are low (<3 cyclones $month^{-1}$), are significant. There is evidence from idealised experiments (Brayshaw et al. 2011) and GCM simulations (O'Reilly et al. 2017; Small et al. 2019) linking the absolute SST and the Gulf Stream SST front sharpness to increased downstream eddy activity. In HadGEM3-GA3.0, the track density increase with resolution is concentrated

Accepted for publication in *Journal of Climate*. DOI10.1175/JCLI-D-19-0054.1.

downstream over the north-eastern North Atlantic and likely driven by the increased sharpness of the OSTIA SST gradients from N96 to N512 (Fig. S1). Increased track density is also simulated over the subtropical Atlantic and northwest Africa at N512, reflecting the detection of vorticity maxima over these lower-latitude regions, where absolute densities are relatively low. A reduction of ETC track density is simulated downstream of orography at N512 compared with N96, particularly over the Northern Mediterranean (downstream of the Alps) and east of southern Greenland (Fig. 6), which is attributable to N512 orography (Fig. S3).

Under RCP8.5, the ensemble-mean spatial response of ETC track density simulated at N96 resolution qualitatively resembles that of the CMIP5 multi-model ensemble (Zappa et al. 2013b): a tri-polar pattern in the track density response is projected over the Euro-Atlantic region, with a decrease over the Mediterranean, increased activity over Northern Europe, particularly the UK and Scandinavia, and decreased track density in high Arctic latitudes (Fig. 7, upper row). Similar responses over northern Europe were simulated by Bengtsson et al. (2006) using ECHAM5. At N512, the magnitude of the ETC track density response is enhanced over northern-western Europe, the western Mediterranean, and the western North Atlantic (Fig. 7, upper row). Under RCP8.5, the ensemble-mean spatial response of ETC mean intensity simulated at N96 resolution is a dipolar pattern, with decreased intensity over the central North Atlantic, western Europe and the Mediterranean, and an increase over the north-eastern North Atlantic and Scandinavia (Fig. 7, lower row). This dipolar spatial structure in ETC intensity response to RCP8.5 is also simulated at N512, but the magnitudes of these responses are enhanced, particularly west of Iberia and north of the United Kingdom and over Scandinavia (Fig. 7, lower row). Consistent with this is an enhanced response in upward vertical velocity (i.e., negative ω) simulated north of ~60 ^{o}N over the north-eastern

Accepted for publication in *Journal of Climate*. DOI10.1175/JCLI-D-19-0054.1.

North Atlantic under RCP8.5 at N512 (Fig. S6), which we attribute to more frequent ETC transits over this region at N512 compared with the lower resolutions based on evidence for moisture-driven ω asymmetry (Tamarin-Brodsky and Hadas 2019).

5. Resolution sensitivity of Euro-Atlantic precipitation under historical climate and RCP8.5

Given that ETCs are the primary contributor to winter precipitation, particularly over Northern Europe (Hawcroft et al. 2012), the resolution-dependence of the simulated ETC track density and mean intensity responses to RCP8.5 is expected to impact projected precipitation. Schiemann et al. (2018) showed that present-climate mean and extreme European precipitation are better represented at N512 (see Supplementary information, section S2, Fig. S7 and Fig. S8), enabling examination of differences in projected precipitation under climate change at each model resolution. To this end, we quantified the impact of increased resolution on ETC-associated and total mean and extreme precipitation in the historical and RCP8.5 HadGEM3-GA3.0 simulations.

5.1 Extratropical cyclone-associated precipitation

Based on tracked ETCs, we decomposed Euro-Atlantic precipitation into cyclone- and non-cyclone-associated components, where the former is determined according to the Hawcroft et al. (2012) method and the latter defined as total minus cyclone-associated precipitation. For the historical climate, as expected, HadGEM3-GA3.0 simulates the highest ETC-associated precipitation values over the storm track region and lower values on the poleward and equatorward flanks of the storm track (Fig. 8). This spatial pattern is consistent across the resolution hierarchy and closely resembles that computed from ERA-Interim (Fig. S9, top

Accepted for publication in *Journal of Climate*. DOI10.1175/JCLI-D-19-0054.1.

399 panel). A negative bias in the magnitude of ensemble-mean ETC-associated precipitation
400 exists over the North Atlantic storm track, which is progressively reduced at N216 and N512
401 resolution, particularly over the downstream storm track region (Fig. S9), highlighting the
402 value of 25 km-resolution in improving the fidelity of simulated precipitation associated with
403 synoptic systems. There are limitations in using ERA-Interim precipitation, which is a
404 forecast, rather than analysed, field. However, Pfahl and Wernli (2012) compared ERA-
405 Interim precipitation flux data with satellite-derived estimates, concluding that, excepting
406 high-intensity events, precipitation sufficiently-well captured by the ERA-Interim forecast
407 model to allow analysis of cyclone-associated precipitation. Use of 6-hourly ERA-Interim
408 precipitation avoids the need to either evaluate HadGEM3-GA3.0 only over the tropical and
409 subtropical regions covered by satellite products or degrade 6-hourly ETC track data to a
410 daily frequency for comparison with global observed precipitation datasets (e.g., GPCP).
411
412 At N512 resolution, significantly higher ETC-associated precipitation is simulated over much
413 of the North Atlantic compared with N96 (Fig. 8), reflecting the spatial pattern of resolution
414 sensitivity in track density (Fig. 6) and corresponding to the region of reduced ETC-
415 associated precipitation bias (Fig. S9). This is also seen over Iberia, the UK, and orographic
416 regions (Scandinavian Mountains and Alps). Significantly reduced ETC-associated
417 precipitation is simulated at N512 over continental mainland Europe and downstream of
418 orography, particularly east of Greenland, the Alps, the Apennines, and the eastern
419 Mediterranean basin (Fig. 8, upper row). The contribution of ETC-associated precipitation to
420 total precipitation in the downstream North Atlantic storm track region and Norwegian Sea is
421 ~5% greater at N512 (Fig. 8, lower row), again reflecting the spatial pattern of resolution
422 sensitivity in ETC track density (Fig. 6) and corresponding to the region of reduced ETC-
423 associated precipitation bias (Fig. S9).

Accepted for publication in *Journal of Climate*. DOI10.1175/JCLI-D-19-0054.1.

Under RCP8.5, CMIP5 models project approximately a doubling of 99th percentile ETC-associated precipitation over eastern North America and northern Europe, but changes over the Mediterranean are comparatively uncertain (Hawcroft et al. 2018). In HadGEM3-GA3.0, ETC-associated precipitation increases under RCP8.5 across north-eastern North America, northern Europe and high-latitude regions, and a significant decrease is simulated over the Mediterranean (Fig. 9). However, increased resolution has little overall impact on these ensemble-mean projections for the North Atlantic, except for orographic European regions (Fig. 9, upper row). The projected contribution of ETC-associated precipitation to total precipitation is reduced across central and southern Europe under RCP8.5 at each resolution (Fig. 9, lower row). Interestingly, a less negative response is simulated over Scandinavia at N512 resolution (Fig. 9) due to the enhanced track density increase under RCP8.5 simulated over this region (Fig. 7). Overall, the ensemble-mean RCP8.5 response is greater than the resolution sensitivity of ETC-associated precipitation by a factor of approximately two. Areas of statistical significance are highly localised, which is a firm indication that, at least in these integrations, ETC track density shifts, rather than changes in mean ETC-associated precipitation, explain spatial patterns of resolution sensitivity in the climate change response of Euro-Atlantic precipitation discussed in section 5.2.

The role of resolution in the simulated response of ETC-associated precipitation to RCP8.5 emerges at smaller spatial scales and when a range of precipitation rates is considered. We quantified the impact of increased resolution on area-averaged ETC-associated precipitation rates over regions where statistically significant changes are projected by CMIP5 as well as in our HadGEM3-GA3.0 simulations: Scandinavia, the UK, Iberia and the Mediterranean. The frequency of ETC-associated precipitation over Scandinavia and the UK simulated at

Accepted for publication in *Journal of Climate*. DOI10.1175/JCLI-D-19-0054.1.

N96 increases under RCP8.5, and a larger increase is simulated at N512 (Fig. 10) for precipitation rates exceeding ~10 mm day^{-1}. These results are consistent with the ECHAM5 simulations of Champion et al. (2011), which showed an increase in the frequency of area-averaged, ETC-associated heavy precipitation events in response to climate change simulated at an atmospheric resolution of 60 km, increasing further at 40 km. However, our results, which span a larger range in resolution, provide evidence that the impact of increasing atmospheric resolution on enhancing the ETC-associated precipitation response over northern Europe is spatially variable. Conversely, the projected decrease in ETC-associated precipitation over Iberia and the Mediterranean under RCP8.5 is indistinguishable between the resolutions considered here. A recent analysis of the added value of high-resolution in simulating present-climate daily precipitation indicates that the coarsest best resolution for the Mediterranean region is uncertain and compounded by observational uncertainty (Roberts et al. 2018).

5.2 Response of European total precipitation to RCP8.5

The CMIP5 multi-model mean response of wintertime mean precipitation to RCP8.5 exhibits a large-scale dipolar pattern of drying across the Mediterranean and southern Europe and wetter conditions across northern Europe (Zappa et al. 2013a). HadGEM3-GA3.0 simulates a similar spatial pattern in both mean and heavy winter precipitation at N96 resolution, which, as expected, resembles that of ETC-associated precipitation (Fig. 11) because ETCs are primarily responsible for mid-latitude precipitation. Increasing resolution from N96 to N216 enhances the RCP8.5 precipitation increase over the Scandinavian mountains and the reduction projected over the Iberian Peninsula and over an area of ocean west of Europe (not shown). Further increasing resolution to N512 enhances this overall dipolar climate change response pattern, particularly over the Norwegian Sea and Iberia (Fig. 11). This enhancement

Accepted for publication in *Journal of Climate*. DOI10.1175/JCLI-D-19-0054.1.

474 of the RCP8.5 response with resolution is significant when tested against interannual
475 variability. Averaged over European sub-regions, interannual variability in total heavy
476 precipitation simulated by HadGEM3-GA3.0 under RCP8.5 is significantly and positively
477 correlated with ETC track density over the eastern North Atlantic at each resolution (Fig.
478 S10), indicating that patterns of resolution-dependence in total precipitation relate directly to
479 changes in upstream ETC activity with resolution. However, this cannot be fully explained by
480 the ETC-associated component of precipitation alone because (i) ETCs are the dominant, but
481 not the only, source of Euro-Atlantic precipitation and (ii) the contribution of ETC-associated
482 precipitation to the total decreases under RCP8.5 in HadGEM3-GA3.0 (Fig. 9). Nevertheless,
483 the mean and heavy precipitation responses simulated at each resolution match those of ETC
484 activity.
485
486 Finally, we computed area-average percentage changes in ETC track density and associated
487 precipitation as well as mean and 95th percentile precipitation (P95) over Scandinavia, the
488 Iberian Peninsula, the Mediterranean, and the UK (Fig. 12). For these regions, we find that
489 area-averaged responses in these quantities simulated at N96 and N512 are generally distinct,
490 but the separation between these resolutions and the intermediate N216 is more variable. For
491 example, the mean precipitation response over Scandinavia shows little change with
492 resolution (Fig. 12a), but responses in P95, ETC frequency and ETC-associated precipitation
493 all increase with resolution (Fig. 12c, d). The track density response for Scandinavia is
494 slightly negative (~-3%) at N96 but positive (~10%) at N512. For Iberia, the RCP8.5
495 response is greater for mean precipitation than P95, but the separation between resolutions is
496 greater for P95. The Iberian P95 change is particularly sensitive to resolution: -12% at N96
497 and -27% at N512. Projected decreases in track density over the Iberia and the Mediterranean
498 at N96 decrease further at N512. These results (i) indicate that ETC-associated precipitation

Accepted for publication in *Journal of Climate*. DOI10.1175/JCLI-D-19-0054.1.

cannot fully explain the overall resolution-dependent precipitation responses to RCP8.5 and (ii) illustrate the complexity of the role of resolution in sub-regional-scale hydroclimate, suggesting the impact-relevance of increased resolution varies spatially.

To summarise, the responses of ETC activity and precipitation to RCP8.5 in HadGEM3-GA3.0 exhibit dipolar spatial patterns generally consistent with CMIP5, but which are enhanced significantly at N512 resolution. This resolution-dependence results from an enhanced poleward shift and downstream, north-eastward extension of both the eddy-driven and subtropical components of the North Atlantic zonal-mean westerly flow simulated at 25 km atmospheric resolution.

6. Discussion

In HadGEM3-GA3.0, the simulated latitudinal distribution of the North Atlantic eddy-driven jet shifts poleward in response to RCP8.5, with corresponding decreases in southern jet occurrences. This poleward shift is more pronounced at N512 compared with N96 (Fig. 1). Eddy-driven jet latitude variability as a function of jet speed decreases under RCP8.5, which is again more pronounced at N512 (Fig. 2). RCP8.5 also engenders a basin-wide, poleward shift in the upper-tropospheric, subtropical component of North Atlantic mean zonal flow (Fig. 4 and Fig. 5). The amplitude of this climate change response is amplified and the eastward jet extension into Europe enhanced by increasing atmospheric model resolution. These large-scale changes have societally-relevant consequences for ETC activity and precipitation over the North Atlantic storm track and Europe.

Accepted for publication in *Journal of Climate*. DOI10.1175/JCLI-D-19-0054.1.

Under RCP8.5, increased (decreased) ETC track density and mean ETC intensity are projected over northern (southern) Europe (Fig. 7). Particularly pronounced changes are projected over Scandinavia and the Iberian Peninsula. Increasing resolution to N512 enhances these regional responses in ETC activity in both the simulated historical (Fig. 6) and future (Fig. 7) climate states. Overall, these spatial patterns of resolution sensitivity in ETC activity under RCP8.5 forcing are explained by the significant poleward shift and eastward extension of the eddy-driven and subtropical components of North Atlantic zonal-mean flow (section 3). However, the ETC activity response to RCP8.5 does not scale linearly with historical ETC activity across resolutions (see Supplementary information, section S3 and Fig. S11). Therefore, several mechanisms governing variability in the position of the North Atlantic jets and storm track, which may be sensitive to atmospheric resolution, may explain the spatial patterns of resolution-dependence seen in this study: changes in meridional temperature gradient (Shaw et al. 2016); tropical forcing by shifts in the Northern Hemisphere Hadley circulation terminus (Tamarin-Brodsky and Kaspi 2017); positive feedback between enhanced latent heating over the north-eastern north Atlantic and increased ETC activity (Willison et al. 2013); or a strengthening of the stratospheric polar vortex (Zappa and Shepherd 2017). Fully evaluating each mechanism is beyond the scope of a single study, so we focus here on meridional temperature gradients. Haarsma et al. (2013) related projected changes in zonal wind to simulated meridional SST gradient changes and CMIP5 simulations have revealed the competing effects of low- versus upper-level meridional temperature gradients in a warming climate on Northern Hemisphere jets (Barnes and Polvani 2015), a key source of uncertainty in future projections. In HadGEM3-GA3.0, the Gulf Stream SST front is more sharply resolved at N512 (Fig. S1) and the overall projected low-level meridional temperature gradient decreases under RCP8.5 due to Arctic amplification, and this decrease is greater at N512 (Fig. S12). However, a significantly

Accepted for publication in *Journal of Climate*. DOI10.1175/JCLI-D-19-0054.1.

548 enhanced meridional temperature gradient, throughout the troposphere and centred at ~50 ºN,
549 is simulated at N512, and this enhancement is most pronounced over the eastern North
550 Atlantic (Fig. S12, lower). We interpret these differences in meridional temperature gradients
551 under RCP8.5 across the HadGEM3-GA3.0 resolution hierarchy to be primarily responsible
552 for the resolution sensitivity in the latitudinal position of the eddy-driven and subtropical jets,
553 which are also more pronounced over the eastern North Atlantic (Fig. 1, Fig. 4 and Fig. 5).
554 We found no evidence for tropical forcing of resolution-dependent zonal wind responses in
555 HadGEM3-GA3.0. The roles of enhanced synoptic activity and diabatic storm track
556 processes feeding back onto the large-scale circulation or by polar vortex changes are
557 priorities for future research.
558
559 Willison et al. (2015) simulated ten initialised January-March seasons (2002-2011) using the
560 Weather Research and Forecast model and perturbed these integrations with the temperature
561 change simulated by five CMIP5 models (including HadGEM2) under RCP8.5, following a
562 modelling approach with similarities to this study (see section 2.1). Willison et al. (2015)
563 identified increased zonal wind and eddy activity under RCP8.5, which was enhanced by
564 increasing resolution from 120 to 20 km, particularly over the north-eastern North Atlantic,
565 consistent with our results (Fig. 7). Willison et al. (2015) used Eulerian storm track metrics to
566 quantify enhanced cyclonic activity over the north-eastern North Atlantic simulated at 20 km
567 resolution, consistent with our results (Fig. 7), but argued for the necessity of Lagrangian
568 feature tracking to fully establish the resolution-dependence of ETC distributions. Our work
569 therefore complements Willison et al. (2015) accordingly and clearly similar spatial patterns
570 of resolution sensitivity emerged when both models were run under the same forcing scenario
571 and span a similar range in atmospheric resolution. Set against a context of previous work
572 showing no significant storm track response to global warming simulated at coarse

Accepted for publication in *Journal of Climate*. DOI10.1175/JCLI-D-19-0054.1.

atmospheric resolutions (Finnis et al. 2007; Matsueda and Palmer 2011), our results provide firm evidence that high-resolution is required to avoid underestimating the magnitude of the response of North Atlantic storm track variability to climate change, with important implications for projecting hazardous weather risk across Europe.

By associating precipitation to tracked ETCs, we isolated the component of total precipitation attributable to ETCs, which exhibits a dipolar response pattern under RCP8.5: wetter (drier) across northern (southern) Europe (Fig. 9), resembling the response of total heavy and mean precipitation (Fig. 11). However, the RCP8.5 response of ensemble-mean ETC-associated precipitation exhibits little change with resolution across Europe. Rather, resolution sensitivity emerges at the sub-regional scale, with north-western European regions showing an enhanced response to RCP8.5 in the tail of area-averaged precipitation rate distributions at N512 (Fig. 10). For northern European regions, however, 25 km-resolution simulations exhibit greater (and reduced biases in) ETC-associated precipitation, indicating that simulations at CMIP5-like resolutions may underestimate the climate change response of this predominant source of European winter precipitation. At 25 km-resolution, the fidelity of simulated precipitation associated with synoptic systems is improved, but precipitation associated with fronts attending ETCs may not be adequately resolved at 25 km. Additionally, no resolution sensitivity is seen for southern Europe sub-regions, at least for the range in resolution considered in this study. We speculate that further increases in resolution to allow convection-permitting integrations are required to make more definitive statements about the role of resolution over southern Europe, a region where mesoscale convective systems are comparatively important for both mean and extreme precipitation (Tous et al. 2016).

Accepted for publication in *Journal of Climate*. DOI10.1175/JCLI-D-19-0054.1.

598 Delworth et al. (2012) simulated an enhanced precipitation increase under a CO_2 doubling
599 scenario over the north-eastern North Atlantic at ~50 km resolution compared with that at
600 ~200 km resolution, consistent with our results, but reduced drying over southern Europe,
601 which is in contrast to our study. However, between these two atmospheric resolutions,
602 Delworth et al. (2012) employed substantially different ocean and land surface model
603 components, obfuscating the role of resolution and reinforcing the necessity for dedicated
604 experiments. In our study, the overall spatial pattern of both the N512 mean and heavy
605 precipitation responses to RCP8.5 and its resolution-dependence (Fig. 11) qualitatively
606 resemble CMIP5 model responses forced by low tropical amplification and a strengthening of
607 the stratospheric polar vortex (Zappa and Shepherd 2017), where the strongest precipitation
608 responses occur over western Europe. Indeed, HadGEM3-GA3.0 simulates both moderately
609 higher tropical Atlantic amplification and an increased strengthening of the stratospheric
610 polar vortex at N512 compared with N96 (not shown), which suggests that this 'storyline'
611 offers dynamical insight into the cause of a resolution-dependent precipitation response to
612 RCP8.5.
613
614
615 **7. Conclusions and outlook**
616 This study quantifies the impact of increasing atmospheric resolution (from ~135 km in the
617 mid-latitudes, which is typical of CMIP5 models, to ~25 km) on the responses of wintertime
618 zonal-mean circulation, ETC activity and precipitation to RCP8.5 across the North Atlantic
619 and Europe. Our analyses are based on an ensemble of atmosphere-only HadGEM3-GA3.0
620 simulations that were experimentally designed for resolution sensitivity studies. We have
621 demonstrated resolution-dependence in North Atlantic zonal-mean circulation, related to

Accepted for publication in *Journal of Climate*. DOI10.1175/JCLI-D-19-0054.1.

differences in meridional temperature gradients, which impacts ETC activity as a function of latitude and, ultimately, downstream precipitation over Europe.

The representation of the North Atlantic eddy-driven jet in HadGEM3-GA3.0 improves when atmospheric horizontal resolution is increased from N96 to N512. Under RCP8.5, a decrease (increase) in the southern (northern) eddy-driven jet regime is projected, as well as a pronounced basin-wide poleward shift in upper-tropospheric zonal flow. These jet responses to warming are significantly enhanced by increased resolution, and related to a more sharply-resolved Gulf Stream SST front and an enhanced low-to-mid-tropospheric meridional air temperature gradient centred at ~50 ºN at N512. The northeast North Atlantic is identified as a region where the increases in ETC activity and precipitation under RCP8.5 are enhanced at N512. Across southern Europe, reduced ETC activity and drying under RCP8.5 are significantly enhanced when resolution is increased. Crucially, reduced ETC track density and ETC-associated precipitation biases at N512 (compared with N96) are co-located with regions where resolution sensitivity in RCP8.5 responses are identified, exemplifying the value of resolving weather-scale processes in a global model to better capture the multi-scale processes important for European climate change projections.

To establish how systematic are these results, a multi-model study conducted under a common experimental protocol is warranted. Future research will exploit a larger ensemble of global climate model simulations, coordinated across multiple European climate modelling centres within the Horizon2020 PRIMAVERA project, which comprises the European submission to CMIP6 HighResMIP (Haarsma et al. 2016). Crucial research directions are establishing the resolution-sufficiency for capturing North Atlantic jet variability and its downstream impact on weather regime frequency and extreme event occurrence over Europe

Accepted for publication in *Journal of Climate*. DOI10.1175/JCLI-D-19-0054.1.

as well as the role of moisture transports coincident with ETC transits, including relatively rare ETCs generated by extratropical transition of tropical cyclones. Moreover, the impact of ocean resolution on the simulated response of Atlantic Meridional Overturning Circulation to climate change and, in turn, on the response of the North Atlantic storm track is under-explored, and HighResMIP offers an opportunity to build on previous analysis of course-resolution (>1°) ocean components of GCMs (Woollings et al. 2012) with evaluations of eddy-resolving and eddy-rich ocean models. Understanding the fundamental physical drivers of the resolution-dependence of North Atlantic circulation, storm activity and precipitation, particularly their responses to climate change, as demonstrated in a global model in this study, may ultimately inform climate risk assessments and the definition of mitigation policies.

Accepted for publication in *Journal of Climate*. DOI10.1175/JCLI-D-19-0054.1.

Author contributions

AJB, RS and PLV conceived the study. AJB performed all data analyses and visualisation and wrote the manuscript. KH developed the cyclone tracking algorithm, *TRACK*, and KH and PLV wrote scripts to post-process *TRACK* output. MED, MSM, MJR, RS, JS and PLV ran the UPSCALE ensemble of simulations. AJB, RS, LES, KH and PLV discussed the results. All authors approved the final manuscript draft.

Acknowledgements

UPSCALE simulations were supported by the PRACE Research Infrastructure (prace-ri.eu) and the Centre for Environmental Data Analysis, which operates the JASMIN platform for data storage and analysis (jasmin.ac.uk). AJB gratefully acknowledges financial support from the PRIMAVERA project, which is funded by the European Commission's Horizon2020 programme (Grant Agreement no. 641727). The authors thank the ENSEMBLES project (ensembles-eu.metoffice.com) for access to the E-OBS dataset, and Benoît Vannière, Giuseppe Zappa, Julia Curio and Robert Lee (National Centre for Atmospheric Science and Department of Meteorology, University of Reading, UK) for helpful discussions. Finally, we are grateful for the time invested in the manuscript by the editor and three anonymous reviewers, whose input much improved the final paper.

Data and code availability

For access to the UPSCALE simulations used in this study, see hrcm.ceda.ac.uk/data. The Met Office Unified Model (MetUM) is available for use under licence. A number of research organisations and national meteorological services use the MetUM in collaboration with the

Accepted for publication in *Journal of Climate*. DOI10.1175/JCLI-D-19-0054.1.

Met Office to undertake basic atmospheric process research, produce forecasts, develop the MetUM code, and build and evaluate Earth system models. For further information, see metoffice.gov.uk/research/collaboration/um-partnership. Version 7.7 of the source code was used in this paper. The Joint UK Land Environment Simulator (JULES) is available under licence. For further information, see jules-lsm.github.io/access_req/JULES_access.html. ERA-Interim data are available from ecmwf.int. TRACK may be obtained from nerc-essc.ac.uk/~kih/TRACK/Track.html. Data analysis and visualisation scripts are available from the lead author upon reasonable request (see also hrcm.ceda.ac.uk/contact).

Accepted for publication in *Journal of Climate*. DOI10.1175/JCLI-D-19-0054.1.

693 **References**

694 Barnes, E. A., and L. M. Polvani, 2015: CMIP5 Projections of Arctic Amplification, of the
695 North American/North Atlantic Circulation, and of Their Relationship. *Journal of Climate*
696 **28,** 5254-5271.

697 Bengtsson, L. et al., 2006: Storm Tracks and Climate Change. *Journal of Climate* **19,** 3518-
698 3543.

699 Brayshaw, D. J. et al., 2011: The Basic Ingredients of the North Atlantic Storm Track. Part II:
700 Sea Surface Temperatures. *Journal of the Atmospheric Sciences* **68,** 1784-1805.

701 Catto, J. L. et al., 2010: Can Climate Models Capture the Structure of Extratropical
702 Cyclones? *Journal of Climate* **23,** 1621-1635.

703 Champion, A. J. et al., 2011: Impact of increasing resolution and a warmer climate on
704 extreme weather from Northern Hemisphere extratropical cyclones. *Tellus A* **63,** 893-906.

705 Dacre, H. F., and S. L. Gray, 2013: Quantifying the climatological relationship between
706 extratropical cyclone intensity and atmospheric precursors. *Geophysical Research Letters* **40,**
707 2322-2327.

708 Dee, D. P. et al., 2011: The ERA-Interim reanalysis: configuration and performance of the
709 data assimilation system. *Quarterly Journal of the Royal Meteorological Society* **137,** 553-
710 597.

711 Della-Marta, P. M., and J. G. Pinto, 2009: Statistical uncertainty of changes in winter storms
712 over the North Atlantic and Europe in an ensemble of transient climate simulations.
713 *Geophysical Research Letters* **36,** L14703.

714 Delworth, T. L. et al., 2012: Simulated Climate and Climate Change in the GFDL CM2.5
715 High-Resolution Coupled Climate Model. *Journal of Climate* **25,** 2755-2781.

716 Demory, M.-E. et al., 2014: The role of horizontal resolution in simulating drivers of the
717 global hydrological cycle. *Climate Dynamics* **42,** 2201-2225.

718 Donlon, C. J. et al., 2012: The Operational Sea Surface Temperature and Sea Ice Analysis
719 (OSTIA) system. *Remote Sensing of Environment* **116,** 140-158.

720 Duchon, C. E., 1979: Lanczos Filtering in One and Two Dimensions. *Journal of Applied*
721 *Meteorology* **18,** 1016-1022.

722 Finnis, J. et al., 2007: Response of Northern Hemisphere extratropical cyclone activity and
723 associated precipitation to climate change, as represented by the Community Climate System
724 Model. *Journal of Geophysical Research: Biogeosciences* **112,** G04S42.

725 Grise, K. M., and L. M. Polvani, 2014: The response of midlatitude jets to increased CO2:
726 Distinguishing the roles of sea surface temperature and direct radiative forcing. *Geophysical*
727 *Research Letters* **41,** 6863-6871.

728 Haarsma, R. J. et al., 2016: High Resolution Model Intercomparison Project
729 (HighResMIP v1.0) for CMIP6. *Geoscientific Model Development* **9,** 4185-4208.

Accepted for publication in *Journal of Climate*. DOI10.1175/JCLI-D-19-0054.1.

730 Haarsma, R. J. et al., 2013: Anthropogenic changes of the thermal and zonal flow structure
731 over Western Europe and Eastern North Atlantic in CMIP3 and CMIP5 models. *Climate*
732 *Dynamics* **41,** 2577-2588.

733 Hawcroft, M. et al., 2018: Significantly increased extreme precipitation expected in Europe
734 and North America from extratropical cyclones. *Environmental Research Letters* **13,** 124006.

735 Hawcroft, M. K. et al., 2012: How much Northern Hemisphere precipitation is associated
736 with extratropical cyclones? *Geophysical Research Letters* **39,** L24809.

737 Hawcroft, M. K. et al., 2016: Can climate models represent the precipitation associated with
738 extratropical cyclones? *Climate Dynamics* **47,** 679-695.

739 Hodges, K. I., 1995: Feature Tracking on the Unit Sphere. *Monthly Weather Review* **123,**
740 3458-3465.

741 Hodges, K. I., 1999: Adaptive Constraints for Feature Tracking. *Monthly Weather Review*
742 **127,** 1362-1373.

743 Hoskins, B. J., 1983: Dynamical processes in the atmosphere and the use of models.
744 *Quarterly Journal of the Royal Meteorological Society* **109,** 1-21.

745 Hoskins, B. J., and K. I. Hodges, 2002: New Perspectives on the Northern Hemisphere
746 Winter Storm Tracks. *Journal of the Atmospheric Sciences* **59,** 1041-1061.

747 Hoskins, B. J. et al., 1983: The Shape, Propagation and Mean-Flow Interaction of Large-
748 Scale Weather Systems. *Journal of the Atmospheric Sciences* **40,** 1595-1612.

749 Huntingford, C. et al., 2014: Potential influences on the United Kingdom's floods of winter
750 2013/14. *Nature Climate Change* **4,** 769.

751 Iqbal, W. et al., 2018: Analysis of the variability of the North Atlantic eddy-driven jet stream
752 in CMIP5. *Climate Dynamics* **51,** 235-247.

753 Kaspi, Y., and T. Schneider, 2013: The Role of Stationary Eddies in Shaping Midlatitude
754 Storm Tracks. *Journal of the Atmospheric Sciences* **70,** 2596-2613.

755 Madonna, E. et al., 2017: The link between eddy-driven jet variability and weather regimes in
756 the North Atlantic-European sector. *Quarterly Journal of the Royal Meteorological Society*
757 **143,** 2960-2972.

758 Masato, G. et al., 2016: A regime analysis of Atlantic winter jet variability applied to
759 evaluate HadGEM3-GC2. *Quarterly Journal of the Royal Meteorological Society* **142,** 3162-
760 3170.

761 Matsueda, M., and T. N. Palmer, 2011: Accuracy of climate change predictions using high
762 resolution simulations as surrogates of truth. *Geophysical Research Letters* **38**.

763 Mizielinski, M. S. et al., 2014: High-resolution global climate modelling: the UPSCALE
764 project, a large-simulation campaign. *Geoscientific Model Development* **7,** 1629-1640.

Accepted for publication in *Journal of Climate*. DOI10.1175/JCLI-D-19-0054.1.

O'Reilly, C. H. et al., 2017: The Gulf Stream influence on wintertime North Atlantic jet variability. *Quarterly Journal of the Royal Meteorological Society* **143,** 173-183.

Pfahl, S. et al., 2017: Understanding the regional pattern of projected future changes in extreme precipitation. *Nature Climate Change* **7,** 423.

Pfahl, S., and H. Wernli, 2012: Quantifying the Relevance of Cyclones for Precipitation Extremes. *Journal of Climate* **25,** 6770-6780.

Pinto, J. G. et al., 2009: Factors contributing to the development of extreme North Atlantic cyclones and their relationship with the NAO. *Climate Dynamics* **32,** 711-737.

Prein, A. F. et al., 2016: Precipitation in the EURO-CORDEX 11° and 44° simulations: high resolution, high benefits? *Climate Dynamics* **46,** 383-412.

Roberts, M. J. et al., 2018: The benefits of global high-resolution for climate simulation: process-understanding and the enabling of stakeholder decisions at the regional scale. *Bulletin of the American Meteorological Society*.

Saha, S. et al., 2010: The NCEP Climate Forecast System Reanalysis. *Bulletin of the American Meteorological Society* **91,** 1015-1058.

Schiemann, R. et al., 2018: Mean and extreme precipitation over European river basins better simulated in a 25km AGCM. *Hydrology and Earth System Sciences* **22,** 3933-3950.

Schneider, T., 2006: The General Circulation of the Atmosphere. *Annual Review of Earth and Planetary Sciences* **34,** 655-688.

Shaw, T. A. et al., 2016: Storm track processes and the opposing influences of climate change. *Nature Geoscience* **9,** 656-664.

Shepherd, T. G., 2014: Atmospheric circulation as a source of uncertainty in climate change projections. *Nature Geoscience* **7,** 703-708.

Small, R. J. et al., 2019: Atmosphere surface storm track response to resolved ocean mesoscale in two sets of global climate model experiments. *Climate Dynamics* **52,** 2067-2089.

Tamarin-Brodsky, T., and O. Hadas, 2019: The Asymmetry of Vertical Velocity in Current and Future Climate. *Geophysical Research Letters* **46,** 374-382.

Tamarin-Brodsky, T., and Y. Kaspi, 2017: Enhanced poleward propagation of storms under climate change. *Nature Geoscience* **10,** 908-913.

Tous, M. et al., 2016: Projected changes in medicanes in the HadGEM3 N512 high-resolution global climate model. *Climate Dynamics* **47,** 1913-1924.

van Haren, R. et al., 2015: Resolution Dependence of European Precipitation in a State-of-the-Art Atmospheric General Circulation Model. *Journal of Climate* **28,** 5134-5149.

Vidale, P. L. et al., 2007: European summer climate variability in a heterogeneous multi-model ensemble. *Climatic Change* **81,** 209-232.

Accepted for publication in *Journal of Climate*. DOI10.1175/JCLI-D-19-0054.1.

Wallace, J. M., and D. S. Gutzler, 1981: Teleconnections in the Geopotential Height Field during the Northern Hemisphere Winter. *Monthly Weather Review* **109,** 784-812.

Walters, D. N. et al., 2011: The Met Office Unified Model Global Atmosphere 3.0/3.1 and JULES Global Land 3.0/3.1 configurations. *Geoscientific Model Development* **4,** 919-941.

Willison, J. et al., 2013: The Importance of Resolving Mesoscale Latent Heating in the North Atlantic Storm Track. *Journal of the Atmospheric Sciences* **70,** 2234-2250.

Willison, J. et al., 2015: North Atlantic Storm-Track Sensitivity to Warming Increases with Model Resolution. *Journal of Climate* **28,** 4513-4524.

Woollings, T., 2010: Dynamical influences on European climate: an uncertain future. *Philosophical Transactions of the Royal Society A: Mathematical, Physical and Engineering Sciences* **368,** 3733.

Woollings, T. et al., 2018: Daily to Decadal Modulation of Jet Variability. *Journal of Climate* **31,** 1297-1314.

Woollings, T. et al., 2012: Response of the North Atlantic storm track to climate change shaped by ocean–atmosphere coupling. *Nature Geoscience* **5,** 313.

Woollings, T. et al., 2010: Variability of the North Atlantic eddy-driven jet stream. *Quarterly Journal of the Royal Meteorological Society* **136,** 856-868.

Zappa, G. et al., 2015: Extratropical cyclones and the projected decline of winter Mediterranean precipitation in the CMIP5 models. *Climate Dynamics* **45,** 1727-1738.

Zappa, G. et al., 2013a: The Ability of CMIP5 Models to Simulate North Atlantic Extratropical Cyclones. *Journal of Climate* **26,** 5379-5396.

Zappa, G. et al., 2013b: A Multimodel Assessment of Future Projections of North Atlantic and European Extratropical Cyclones in the CMIP5 Climate Models. *Journal of Climate* **26,** 5846-5862.

Zappa, G., and T. G. Shepherd, 2017: Storylines of Atmospheric Circulation Change for European Regional Climate Impact Assessment. *Journal of Climate* **30,** 6561-6577.

Zhang, L. et al., 2016: Added value of high resolution models in simulating global precipitation characteristics. *Atmospheric Science Letters* **17,** 646-657.

Zveryaev, I. I., 2004: Seasonality in precipitation variability over Europe. *Journal of Geophysical Research: Atmospheres* **109,** D05103.

Zveryaev, I. I., 2006: Seasonally varying modes in long-term variability of European precipitation during the 20th century. *Journal of Geophysical Research: Atmospheres* **111,** D21116.

Accepted for publication in *Journal of Climate*. DOI10.1175/JCLI-D-19-0054.1.

Figures

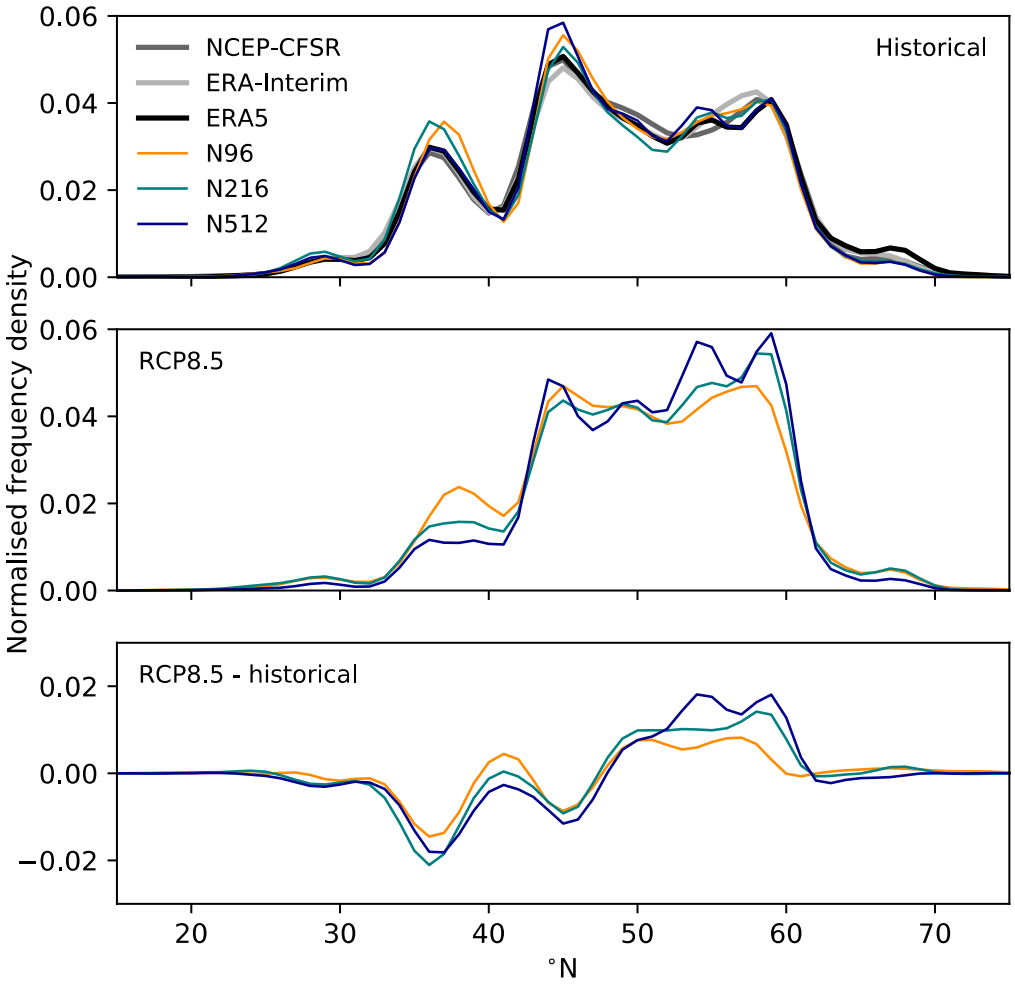

Fig. 1. Regime behaviour of the North Atlantic eddy-driven jet stream, measured by jet latitude, as represented in the ERA5 (black), ERA-Interim (pale grey) and NCEP-CFSR (grey) reanalyses and simulated by HadGEM3-GA3.0 for (upper panel) historical climate, (middle panel) under RCP8.5, and (lower panel) the difference (i.e., RCP8.5 minus historical; lower panel). At each model resolution, N96 (orange), N216 (teal) and N512 (blue) ensemble members were concatenated to maximise sampling. Unit is normalised frequency density and plotted as a function of latitude. In the lower panel, frequency = 0 (horizontal black line) is shown.

Accepted for publication in *Journal of Climate*. DOI10.1175/JCLI-D-19-0054.1.

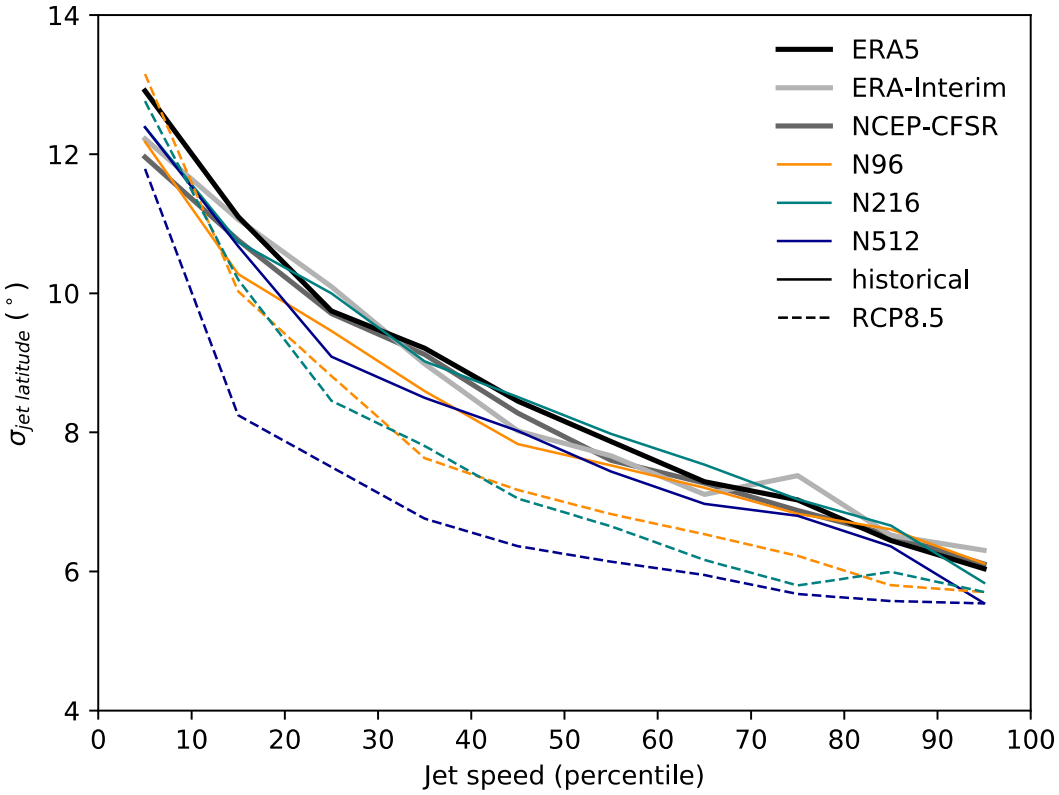

846

847 **Fig. 2.** Variance in North Atlantic eddy-driven jet stream latitude ($\sigma_{jet\ latitude}$) as a function of
848 jet speed, as represented in the ERA5 (black), ERA-Interim (pale grey) and NCEP-CFSR
849 (grey) reanalyses and simulated by HadGEM3-GA3.0. In this analysis, the standard deviation
850 of daily jet latitude is binned according to jet speed (shown as percentiles) with a bin width of
851 10 %, following Woollings et al. (2018). Curves for the historical climate (solid lines) and
852 RCP8.5 (dashed lines) integrations at N96 (orange), N216 (teal) and N512 (blue) resolutions
853 were constructed by concatenating ensemble members to maximise sampling.

854

Accepted for publication in *Journal of Climate*. DOI10.1175/JCLI-D-19-0054.1.

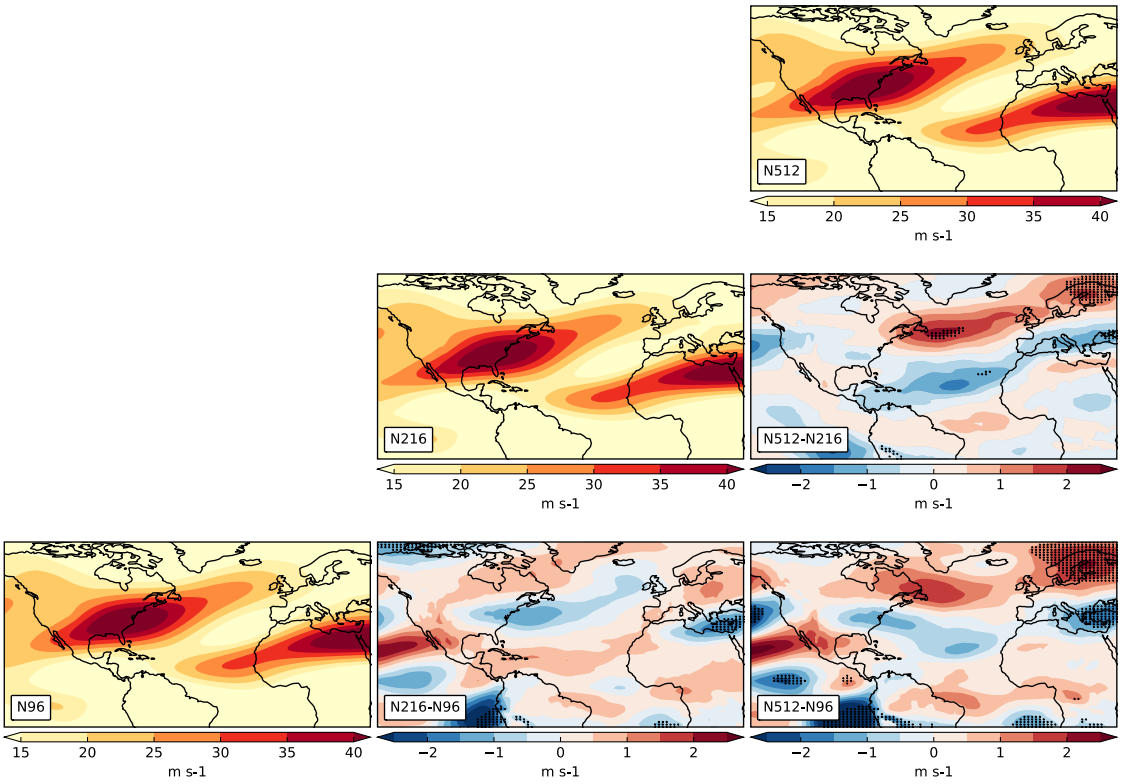

855

856 **Fig. 3.** Resolution sensitivity of the ensemble-mean upper-tropospheric (250 hPa) winter

857 westerly zonal wind over the North Atlantic under historical SST forcing (1985-2011). N96

858 (lower-left), N216 (centre) and N512 (upper-right), with corresponding resolution differences

859 (lower-right panels). Stippling indicates statistically significant resolution differences at the

860 95% level. Unit is m s^{-1}.

861

Accepted for publication in *Journal of Climate*. DOI10.1175/JCLI-D-19-0054.1.

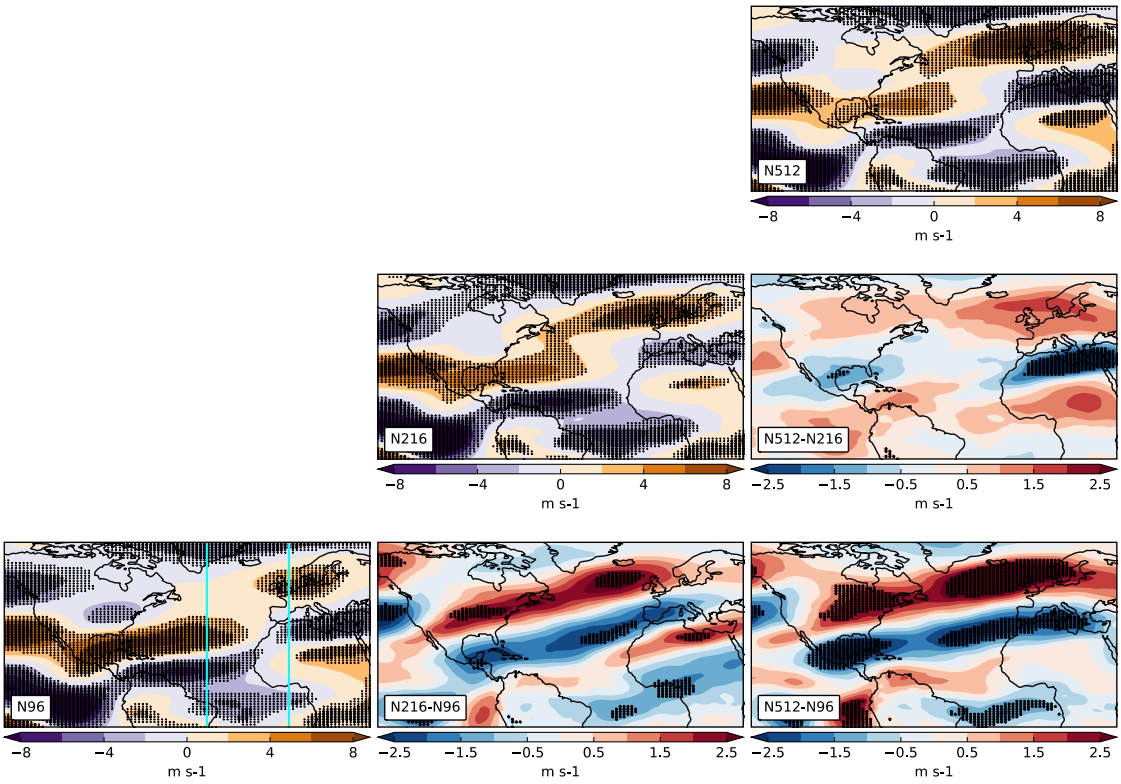

862

863 **Fig. 4.** Resolution sensitivity of the ensemble-mean upper-tropospheric (250 hPa) winter

864 westerly zonal wind response to RCP8.5 over the North Atlantic. Panel layout as per Fig. 3.

865 The vertical cyan lines drawn at 40ºW and 0º in the N96 panel indicate the sector averaged in

866 Fig. 5. Stippling indicates that the climate change response or resolution difference is

867 statistically significant at the 95% level. Unit is m s^{-1}.

868

Accepted for publication in *Journal of Climate*. DOI10.1175/JCLI-D-19-0054.1.

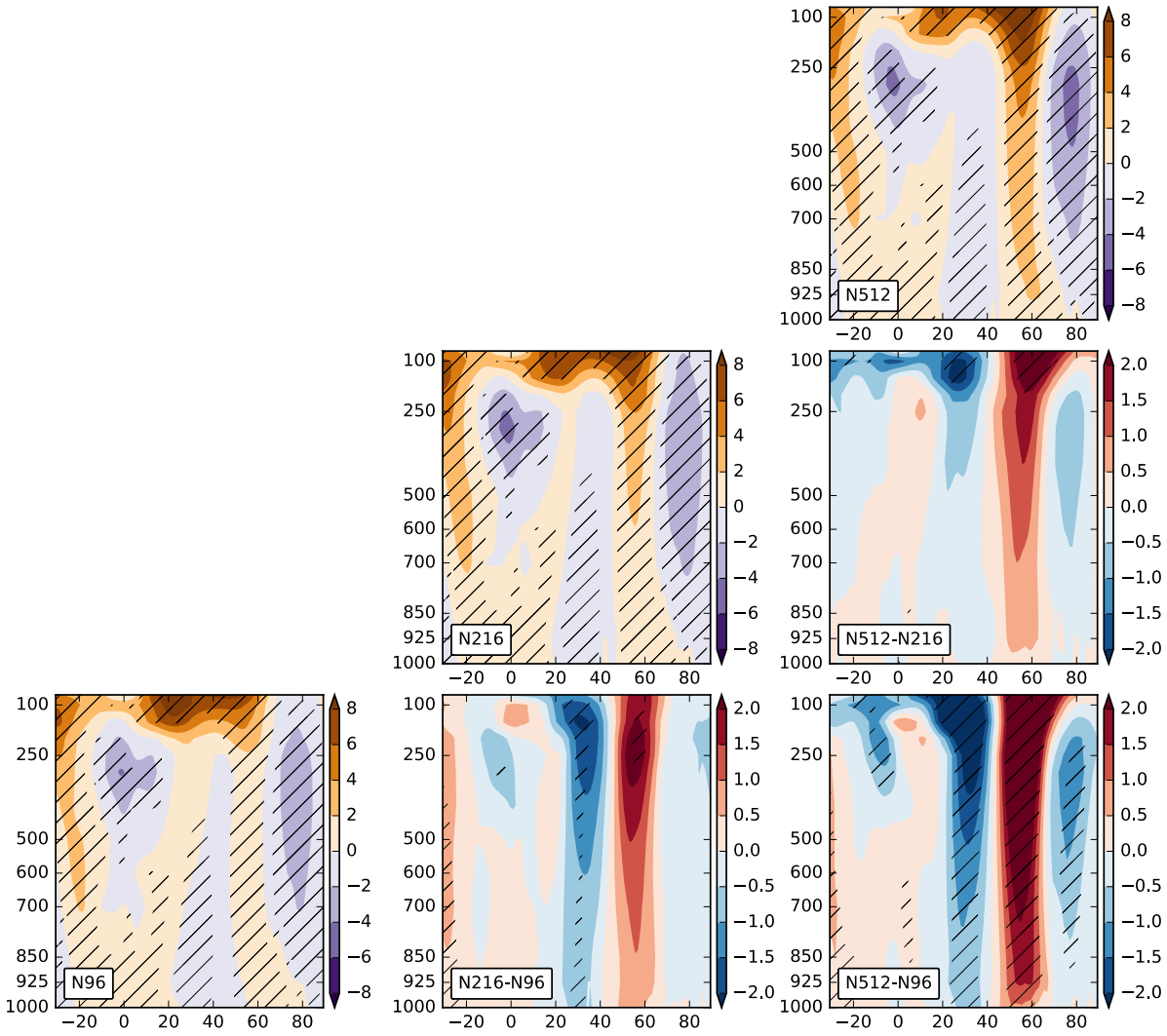

Fig. 5. Vertical profile of the ensemble-mean winter westerly zonal wind response to RCP8.5, averaged zonally over the eastern North Atlantic between 0° and 40°W. Panel layout as per Fig. 3. Note that the vertical pressure axis is linear but only certain conventional pressure levels are labelled (in hPa) for clarity. Diagonal hatching indicates that the climate change response or resolution difference is statistically significant at the 95% level. Unit is m s^{-1}.

Accepted for publication in *Journal of Climate*. DOI10.1175/JCLI-D-19-0054.1.

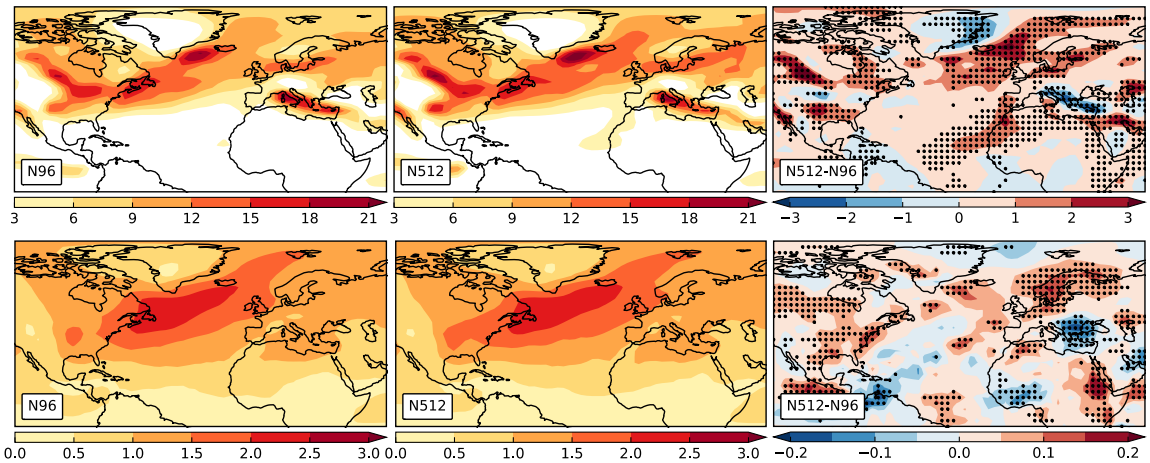

878

879 **Fig. 6.** Resolution sensitivity of ensemble-mean North Atlantic winter storm track, as
880 measured by ETC track density (upper row) and mean ETC vorticity intensity (lower row)
881 for historical climate simulations (1986-2011). Shown are N96 (left), N512 (middle) and the
882 difference between these resolutions (right). Track density unit is cyclone transits per month
883 per unit area (equivalent to a cyclone-centred 5° spherical cap). Mean intensity unit is
884 vorticity scaled by 10^5 s^{-1}. Stippling indicates statistically significant resolution differences at
885 the 95% level.

886

Accepted for publication in *Journal of Climate*. DOI10.1175/JCLI-D-19-0054.1.

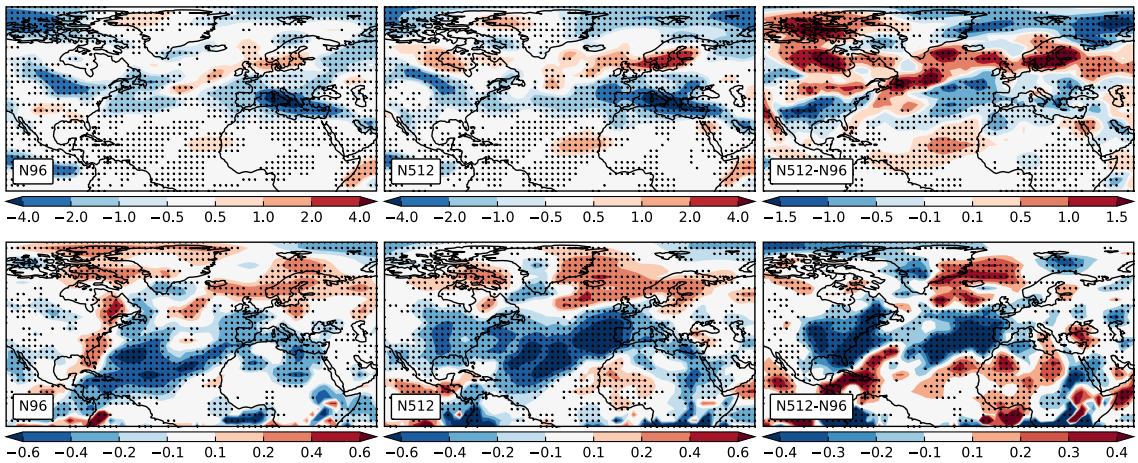

887

888 **Fig. 7.** Resolution sensitivity of the ensemble-mean response of winter ETC track density
889 (upper row) and mean intensity (lower row) to the RCP8.5 scenario over the North Atlantic.
890 Panel layout as per Fig. 6. Stippling indicates that the climate change response or resolution
891 sensitivity is statistically significant at the 95% level. Track density unit is cyclone transits
892 per month per unit area (equivalent to a cyclone-centred 5° spherical cap). Mean intensity
893 unit is vorticity scaled by 10^5 s^{-1}.

894

Accepted for publication in *Journal of Climate*. DOI10.1175/JCLI-D-19-0054.1.

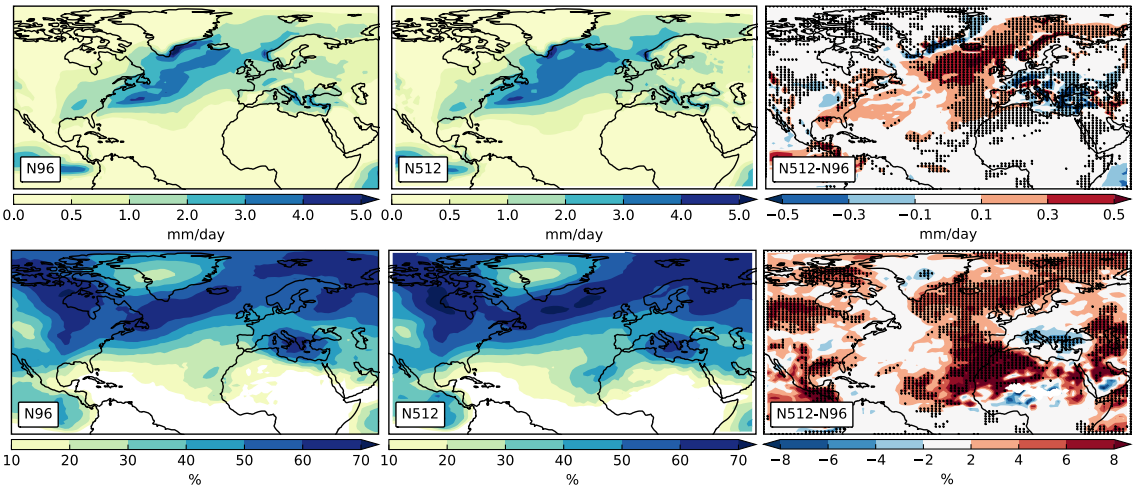

Fig. 8. Resolution sensitivity of ensemble-mean North Atlantic winter ETC-associated precipitation (upper row) and ETC contribution to total precipitation (lower row) for historical climate simulations (1986-2011). Panel layout as per Fig. 6. Stippling indicates statistically significant resolution sensitivity at the 95% level. Units are mm day^{-1} and %, respectively.

Accepted for publication in *Journal of Climate*. DOI10.1175/JCLI-D-19-0054.1.

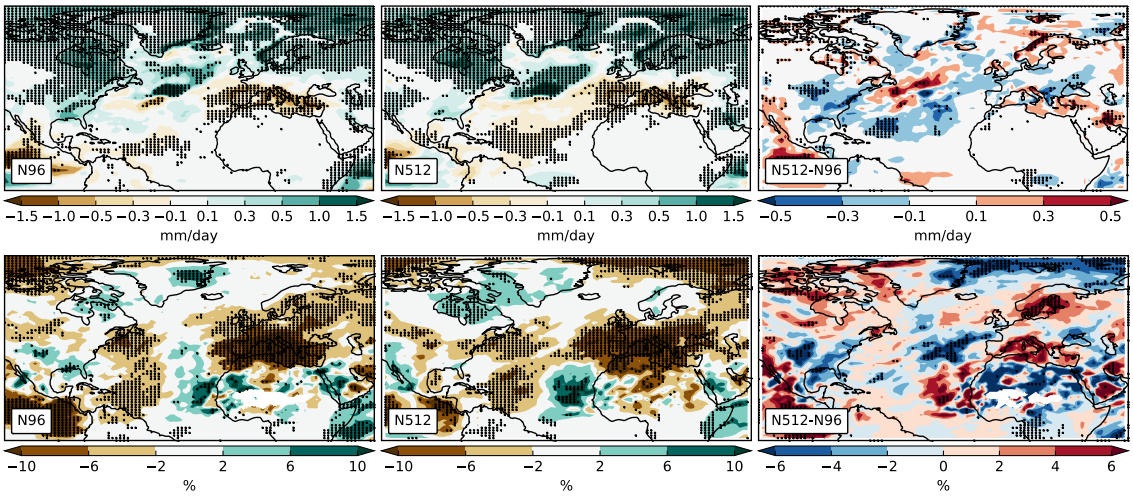

902

903 **Fig. 9.** Resolution sensitivity of the responses of ensemble-mean North Atlantic winter ETC-
904 associated precipitation (upper row) and ETC contribution to total precipitation (lower row)
905 to RCP8.5. Panel layout as per Fig. 6. Stippling indicates that the climate change response or
906 resolution sensitivity is statistically significant at the 95% level. Units are mm day^{-1} and %,
907 respectively.

908

Accepted for publication in *Journal of Climate*. DOI10.1175/JCLI-D-19-0054.1.

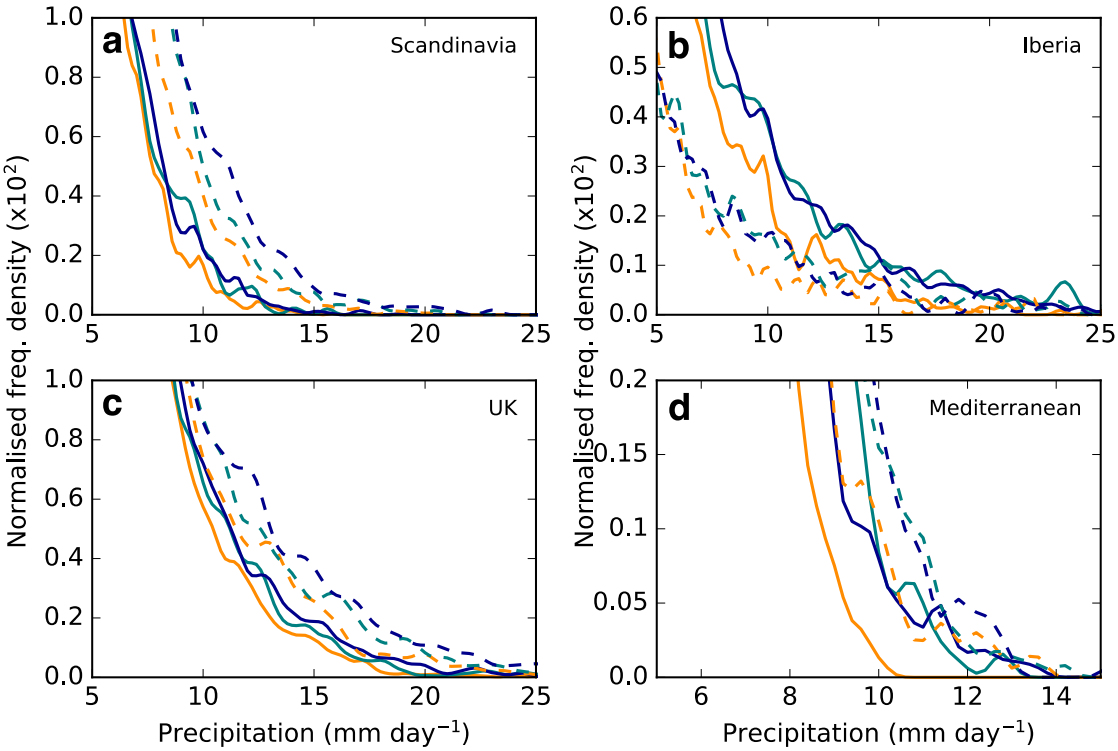

909

910 **Fig. 10.** Domain-mean frequency distribution of ETC-associated precipitation over (a)

911 Scandinavia, (b) Iberia, (c) the UK, and (d) the Mediterranean under historical (solid lines)

912 and RCP8.5 forcing (dashed lines). Ensemble members were concatenated to maximise

913 sampling of high precipitation rates. Colours are as per Fig. 1.

914

Accepted for publication in *Journal of Climate*. DOI10.1175/JCLI-D-19-0054.1.

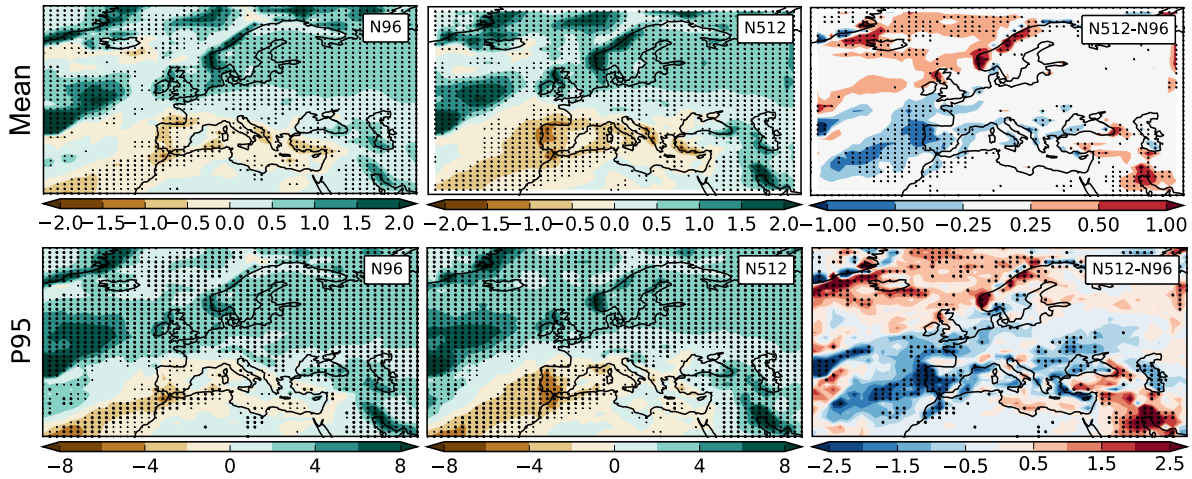

915

916 **Fig. 11.** Resolution sensitivity of ensemble-mean winter mean (upper row) and 95th percentile
917 (lower row) precipitation response to RCP8.5 over Europe. Panel layout as per Fig. 6.
918 Stippling indicates statistically significant climate change response or resolution sensitivity at
919 the 95% level. Unit is mm day^{-1}.

920

Accepted for publication in *Journal of Climate*. DOI10.1175/JCLI-D-19-0054.1.

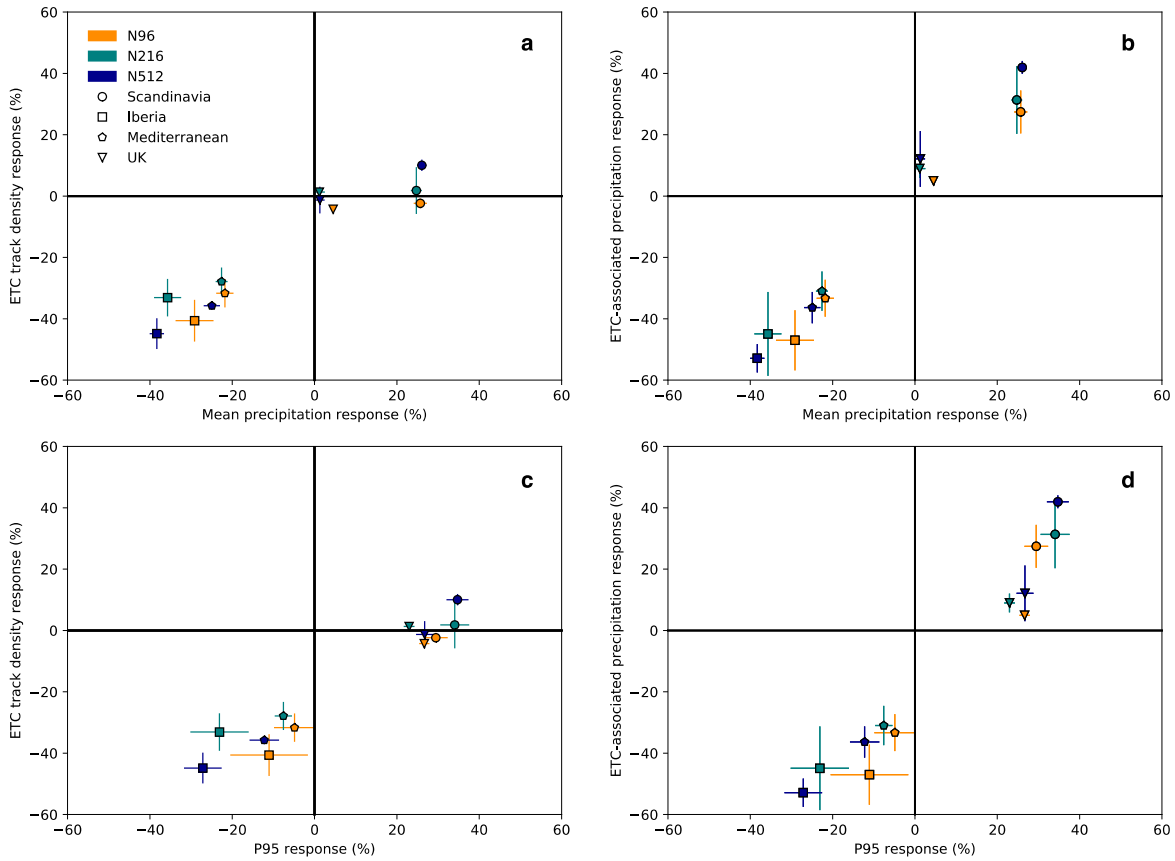

921

922 **Fig. 12.** Area-weighted, domain-mean percentage change of ETC track density and ETC-
923 associated precipitation under RCP8.5 as a function of (a,b) mean and (c,d) 95th percentile
924 precipitation for each HadGEM3-GA3.0 resolution. Markers indicate the ensemble mean and
925 error bars indicate the standard deviation of the ensemble members. The RCP8.5 response of
926 each individual future climate ensemble member is computed as a percentage difference from
927 the present-climate ensemble mean.

928

Accepted for publication in *Journal of Climate*. DOI10.1175/JCLI-D-19-0054.1.